



Article

Spatial Distribution of Cropping Systems in South Asia Using Time-Series Satellite Data Enriched with Ground Data

Murali Krishna Gumma ^{1,*}, Pranay Panjala ¹, Sunil K. Dubey ², Deepak K. Ray ³, C. S. Murthy ², Dakshina Murthy Kadiyala ⁴, Ismail Mohammed ¹ and Yamano Takashi ⁵

¹ International Crops Research Institute for the Semi-Arid Tropics (ICRISAT), Patancheru 502324, India; pranay.panjala@icrisat.org (P.P.)

² Mahalanobis National Crop Forecast Centre (MNCFC), New Delhi 110012, India

³ Institute on the Environment, University of Minnesota, St. Paul, MN 55108, USA

⁴ Department of Agronomy, Acharya NG Ranga Agricultural University, Guntur 522034, India

⁵ Asian Development Bank, Dhaka 1207, Bangladesh

* Correspondence: muralikrishna.gumma@icrisat.org or gummamk@gmail.com

Abstract: A cropping system practice is the sequential cultivation of crops in different crop seasons of a year. Cropping system practices determine the land productivity and sustainability of agriculture in regions and, therefore, information on cropping systems of different regions in the form of maps and statistics form critical inputs in crop planning for optimal use of resources. Although satellite-based crop mapping is widely practiced, deriving cropping systems maps using satellites is less reported. Here, we developed moderate-resolution maps of the major cropping systems of South Asia for the year 2014–2015 using multi-temporal satellite data together with a spectral matching technique (SMT) developed with an extensive set of field observation data supplemented with expert-identified crops in high-resolution satellite images. We identified and mapped 27 major cropping systems of South Asia at 250 m spatial resolution. The rice-wheat cropping system is the dominant system, followed by millet-wheat and soybean-wheat. The map showing the cropping system practices of regions opens up many use cases related to the agriculture performance of the regions. Comparison of such maps of different time periods offers insights on sensitive regions and analysis of such maps in conjunction with resources maps such as climate, soil, etc., enables optimization of resources vis-à-vis enhancing land productivity. Thus, the current study offers new opportunities to revisit the cropping system practices and redesign the same to meet the challenges of food security and climate resilient agriculture.

Keywords: cropping systems; South Asia; crop type mapping; time-series analysis; crop phenology detection



Citation: Gumma, M.K.; Panjala, P.; Dubey, S.K.; Ray, D.K.; Murthy, C.S.; Kadiyala, D.M.; Mohammed, I.; Takashi, Y. Spatial Distribution of Cropping Systems in South Asia Using Time-Series Satellite Data Enriched with Ground Data. *Remote Sens.* **2024**, *16*, 2733. <https://doi.org/10.3390/rs16152733>

Received: 16 May 2024

Revised: 16 July 2024

Accepted: 16 July 2024

Published: 26 July 2024



Copyright: © 2024 by the authors. Licensee MDPI, Basel, Switzerland. This article is an open access article distributed under the terms and conditions of the Creative Commons Attribution (CC BY) license (<https://creativecommons.org/licenses/by/4.0/>).

1. Introduction

A cropping system indicates the crop types and sequences practiced in a region over the crop seasons of a year. Generally, a crop year consists of multiple crop seasons of roughly defined duration. The crops grown during these seasons comprise the cropping system of that region, characterizing the agricultural practices followed in that area as a whole rather than in an individual parcel of land. In India, there are three crop seasons: *kharif* (June to November), *rabi* (November to March) and *zaid* (March to June). Crops are grown in one, two or all three of these seasons, with variations from region to region. For instance, if rice is grown in the initial season followed by wheat in the second season and no crop in the third, then it is called a rice-wheat cropping system. The agroecological and agrometeorological conditions of a region have a bearing on the cropping system practiced there.

Cropping systems play a role in determining the land productivity of a region by facilitating optimal utilization of resources to maximize crop yields [1]. However, resource-intensive cropping systems tend to impact soil health, ground and surface-water hydrology,

environmental sustainability, climate resilience of agriculture and income security of farmers. Sustainable agriculture is closely linked to cropping system practices [2,3]. Therefore, monitoring cropping systems is of critical importance to sustainable agriculture and food production. In particular, cropping system maps can provide important information on crop types, the number of crops grown and the management practices followed in irrigated or rainfed systems during a crop year at a particular location. Given the growing population and rapid climate change, there is increasingly a need to monitor and reduce emissions in the quest for sustainable agriculture development.

Cereals and legumes, especially short-duration crops, are crucial for food and nutrition security in Asia and Africa. They have the potential to improve livelihoods by enhancing incomes and providing stable employment. However, increasing cropping intensity through better irrigation technology, fertilizer use and mechanization has led to growing pressure on croplands and other environmental concerns. The need to allocate water to other competing sectors (urban and industrial development) and reduced water availability in a highly varying climate inhibit the expansion of irrigated cropland area [4,5]. Additionally, the adverse impacts of accelerated irrigation development and fertilizer use have been manifest in increasing salinity in croplands, leading to loss of soil fertility.

Given that context, mapping cropping systems can provide a crucial input into decision-making to improve cropping systems, explore opportunities to increase production and raise farmers' incomes under conditions where there can be no further expansion of agricultural area. Additionally, accurate crop information from the lowest administrative level is necessary to estimate country-level crop-wise acreage [6–8], which is a basic input that feeds into agricultural policies. Since dryland cropping systems are highly mutable and are influenced by biophysical, social and economic factors [9–12], accurate estimation of cropping patterns is essential for planning. In such a scenario, geospatial products can provide input parameters for food security studies, and also for developing seasonal cropping patterns of cereals followed by short-duration legumes [13,14].

There is a need to revisit the cropping system practices of different regions in view of the growing importance of sustainable agriculture and food systems. With climate change leading to increased exposure of agriculture to various risks, and fast-changing food habits altering the demand and supply scenario of food, there is increasing recognition of the importance of carbon-neutral economies and also reassessment of the global trade practices. Mapping and inventory taking of croplands following different cropping systems are basic information products that can aid in the development of more suitable cropping systems in different regions. Spatial information on current cropping systems integrated with layers of information on resources such as soil, weather and water will enable a holistic assessment of the sustainability of current agricultural systems.

There have been numerous studies on mapping cropping patterns using satellite data, but they are limited to the subdistrict and plot levels [15–17] and single or major crops at large scale such as rice, wheat and sugarcane [18–22]. Currently, the various data sources available for use include regional and subnational statistical data on cultivated areas, coarse/medium-scale land-use/land-cover (LULC) maps and paddy maps from the 1980s to the 2010s [23–25], maps of rice areas using medium spatial resolution data [19,26–28] and a combination of various other sources [29,30].

Modern remote sensing is characterized by frequent imaging of the earth's surface to produce large streams of spectral data in high to moderate resolutions and making available analysis-ready data and biophysical products in the public domain to map agriculture systems. These developments in remote sensing offer numerous opportunities to produce more accurate and customized information on crop cover and its changes.

Information on spatial distribution of different cropping systems is important for spatial analysis to identify areas appropriate for sustainable food production, for a better understanding of where croplands are available to introduce/grow short-duration legumes across winter fallows, and to overcome current farmers' income uncertainties. Analysis of near-real-time satellite imagery can be a substitute for ground surveys to estimate the acreage of major crop

types; moreover, it is relatively quick, cheap and independent [31–35]. Some studies have used satellite data to map agricultural areas at various temporal and spatial resolutions [36–41]; moderate resolution imaging spectrometer (MODIS) normalized difference vegetation index (MODIS NDVI) time-series data to map croplands, cropping intensity at lower administrative levels and for river basins [42–44]; and land surface water index (LSWI) data to monitor natural vegetation- and soil-related wetness at a regional scale [26,45–48].

However, to our knowledge, none of these studies have dealt with entire cropping systems, i.e., crops grown in a sequence over the entire year. This study maps major cropping systems across South Asia with the help of MODIS time-series data and spectral matching techniques (SMTs) to provide precise information on cropping sequences with the objective of enabling improvement of crop water productivity and proper natural resource management.

2. Materials and Methods

2.1. Study Area

South Asia is located between $5^{\circ}38'$ and $36^{\circ}54'N$ latitudes and $61^{\circ}05'$ and $97^{\circ}14'E$ longitudes, covering nearly 477 million ha. The region comprises Bangladesh, Bhutan, India, Nepal, Pakistan and Sri Lanka (Figure 1), and is divided, based on similar climatic conditions, into six agroecological zones (AEZs) [49] in which agriculture is strongly influenced by rainfall and seasonal winds. South Asia is home to 65% of the underprivileged people who live in rural and remote areas and depend on agriculture for their livelihood [50]. People living in 70% of the countryside depend on coastal fisheries and land. South Asia has nine major river basins: Brahmaputra, Godavari, Indus, Ganges, Tapti, Krishna, Kaveri, Narmada and Mahanadi. Irrigation projects in this region serve a command area of nearly 133 million ha [51]. Rice and wheat are the staple foods in the region; the former crop is grown throughout the year in some areas.

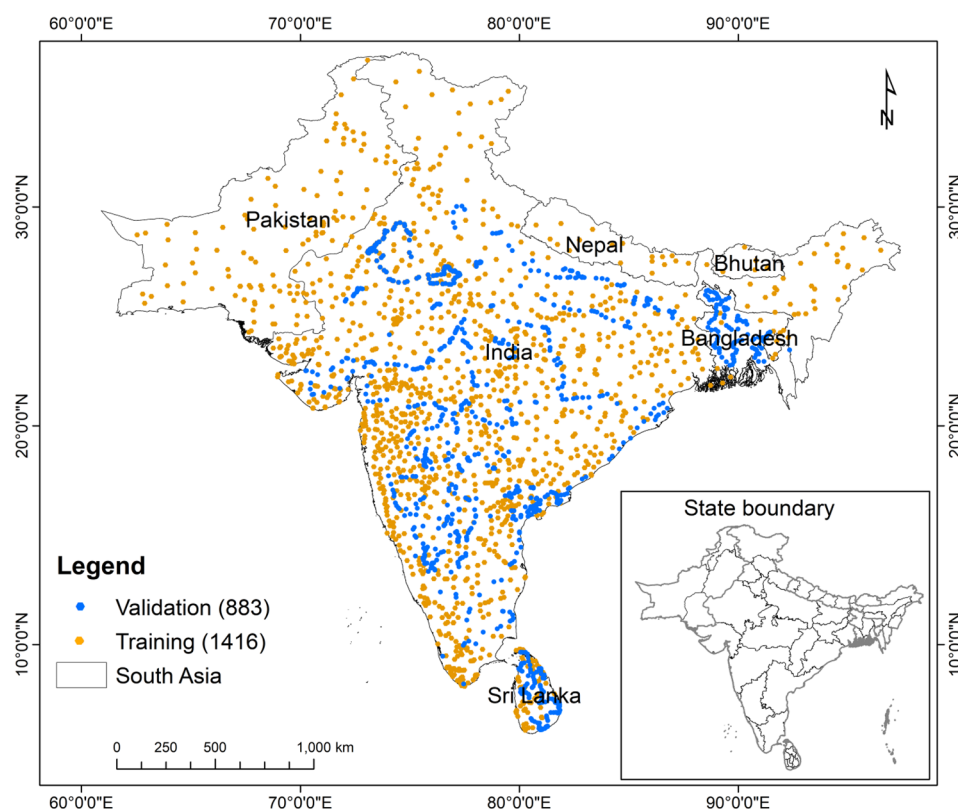


Figure 1. Spatial distribution of ground data collected for the crop year 2014–2015.

The major cropping systems in South Asia vary by country (Table 1). India has diversified cropping systems, but rice-wheat is dominant in northern India and rice-rice in

southern India. In Sri Lanka, rice-rice, rice-fallow and other crops-fallow are the dominant cropping systems. In Bangladesh, rice-rice, rice-pulses-rice, rice-fallow-rice and jute-pulses-rice are popular; Bhutan favors rice-fallow and mixed crops. The dominant cropping systems in Nepal are rice-wheat, maize-wheat and maize-rice, whereas in Pakistan they are rice-wheat, rice-rice, rice-pulses and cotton. Thus, rice-rice and rice-wheat are the common major cropping systems across the region.

Table 1. Country-wise major cropping systems in South Asia.

Country	Total Geographical Area ('000 ha)	Total Gross Planted Area ('000 ha)	Major Cropping Systems
Bangladesh	14,804	15,002	Rice-rice, rice-pulses-rice, rice-fallow-rice, jute-pulses-rice
Bhutan	4365	121	Rice-fallow, mixed crops
India	345,623	184,443	Diversified cropping systems (Table 2)
Nepal	16,210	4208	Rice-wheat, maize-wheat, maize-rice
Pakistan	89,167	22,817	Rice-wheat, rice-rice, rice-pulses, cotton
Sri Lanka	6453	2076	Rice-rice, rice-fallow, other crops-fallow
Total	476,622	228,668	

Note: The gross planted area indicates the total sown area within a crop year, including multiple cropping cycles where applicable.

Table 2. Field samples used for training and validation, and national statistics on cropping systems in India.

Classified Data	Training Samples	Validation Samples	Cropping Systems in India (M ha)
01. Rice-wheat	42	46	14.8
02. Rice-rice	15	88	2.4
03. Rice-pulses	18	51	4
04. Pulses/rice-rice	13	107	4.5
05. Soybean-wheat	18	33	8.3
06. Pulses-wheat	17	22	9.2
07. Maize-wheat	35	24	NA
08. Millet-wheat	53	38	10.1
09. Maize-wheat	3	13	2.5
10. Maize-chickpea	16	14	4
11. Millet-mustard	10	20	3.8
12. Pulses-maize	9	10	2
13. Sugarcane	22	17	5.1
14. Groundnut-pulses	7	15	4
15. Sorghum-fallow	9	18	1.3
16. Rice-fallow	23	58	12.6
17. Pigeonpea-fallow	28	27	5.5
18. Groundnut/cotton	9	15	NA
19. Cotton-fallow	77	43	15.3
20. Millet-fallow	18	13	3.8
21. Sorghum-fallow	19	16	3.2
22. Pulses-fallow	9	11	1.3
23. Fallow-chickpea	4	16	1.4
24. Groundnut-fallow	18	14	9.7
25. Mixed crops	94	55	NA
26. Other LULC	773	61	NA
27. Rice-fallow/mixed crops	57	38	NA
Total samples	1416	883	

2.2. Ground Reference Data

Ground survey information with geographical coordinates (Table 2) was collected broadly throughout South Asia for the crop year 2014–2015 for identification of classes of cropping systems together with an accuracy assessment exercise (Figure 1). Ground data collection was conducted using two distinct approaches. For the training data, homogeneous patches were selected, and comprehensive crop-related information was collected to generate ideal spectra signatures. In contrast, the validation data were gathered from various random locations, focusing primarily on land use, land cover, crop name rather than detailed information. A total of 2203 field samples were collected, of which 1416 points

were used for training to develop an ideal spectral data bank (ISDB) and 883 for class validation (Table 2). Land-use land-cover information was collected for each sample (at least 250 m × 250 m) along with data on crop type, cropping intensity and irrigation water source. During collection of ground data, the area around the sample was categorized into one of three classes: small (≤ 10 ha); medium (10–15 ha); and large (≥ 15 ha) to enable acreage estimation. In some areas, farmers were interviewed to glean information on sowing dates, irrigation practices and cropping patterns to aid class identification. For areas that could not be visited due to lack of proper roads, information was obtained from secondary sources, including local agriculture experts and records. Class names were allotted in the field using a labeling protocol [31,52]. Data limitations in some areas led to classes being identified on the basis of prior experience with crop signatures.

Data on India's agriculture were obtained from the official websites of the Department of Agriculture of the Government of India; other countries' data were obtained from the respective national agricultural/statistics departments.

As per Indian national statistics, the dominant rainfed cropping systems are cotton-fallow (15.3 M ha) followed by rice-fallow (12.6 M ha) and groundnut-fallow (9.7 M ha). The major irrigated cropping systems are rice-wheat (14.8 M ha) followed by millet-wheat (10.1 M ha). The other major cropping systems are pulses-wheat (9.2 M ha) and soybean-wheat (8.3 M ha) (Table 2).

3. Methodology

The workflow of this study consisted of three major steps: (1) preparation of satellite data including mosaicking and stacking; (2) running the machine learning algorithm, i.e., unsupervised classification (K-means) on Google Earth Engine (GEE) and identification of classes and labeling with the help of SMTs; and (3) accuracy assessment using validation data and national statistics (Figure 2).

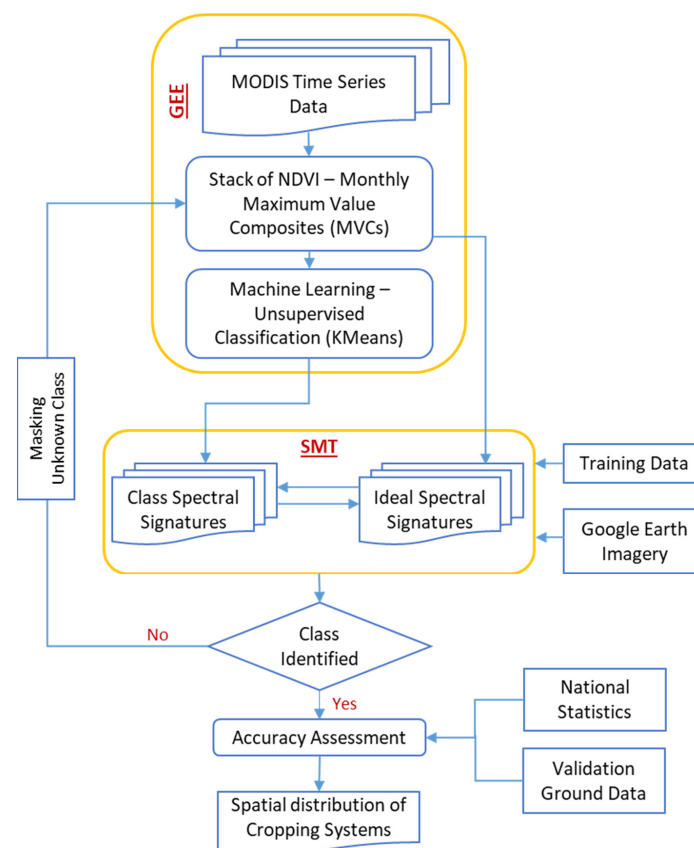


Figure 2. The steps to map crop dominance classification.

3.1. Preparation of Satellite Data and Running Machine Learning Algorithm

In GEE, the readily available MOD13Q1 V6.1 product provides preprocessed NDVI data for every 16 days on a per-pixel basis, masked for water, clouds, heavy aerosols and cloud shadows. Twelve MODIS tiles covering the study area for the study year June 2014–May 2015 were considered for our analysis.

The monthly maximum NDVI imagery was calculated using Equation (1).

$$NDVIMVC_i = \text{Max}(NDVI_{i1}, NDVI_{i2}) \quad (1)$$

where, MVC_i = Month maximum composite of i^{th} month (e.g., “i” is June–May) and $i_1, i_2 = 16$ -day images in a month.

The images were first stacked as monthly maximum-value composites, which means that the maximum NDVI values for every month were stacked for the study year 2014–15, making an analysis-ready data (ARD) cube of 12 months, one for each month, thus providing the NDVI variation in a crop year and overall coverage of the whole study area. MODIS data has temporal resolution of one day. Since this study considered monthly maximum images, there was less chance of missing pixel values; in an exceptional case, linear regression interpolation was done to fill the gap.

The final ARD cube was set into a K-means unsupervised machine learning algorithm with 100 clusters for every agroecological zone. The machine learning algorithm classifies the ARD cube into 100 clusters with 100 class spectral signatures.

3.2. Spectral Matching Techniques for Class Identification and Labeling

3.2.1. Ideal Spectral Signatures (ISS)

Ideal spectral signatures for cropping systems were generated based on independent training data drawn from extensive field survey information using time-series data. The ground samples were grouped based on their distinctive characteristics and later classified into classes of unique cropping systems. Figure 3 shows the ISS of various classes.

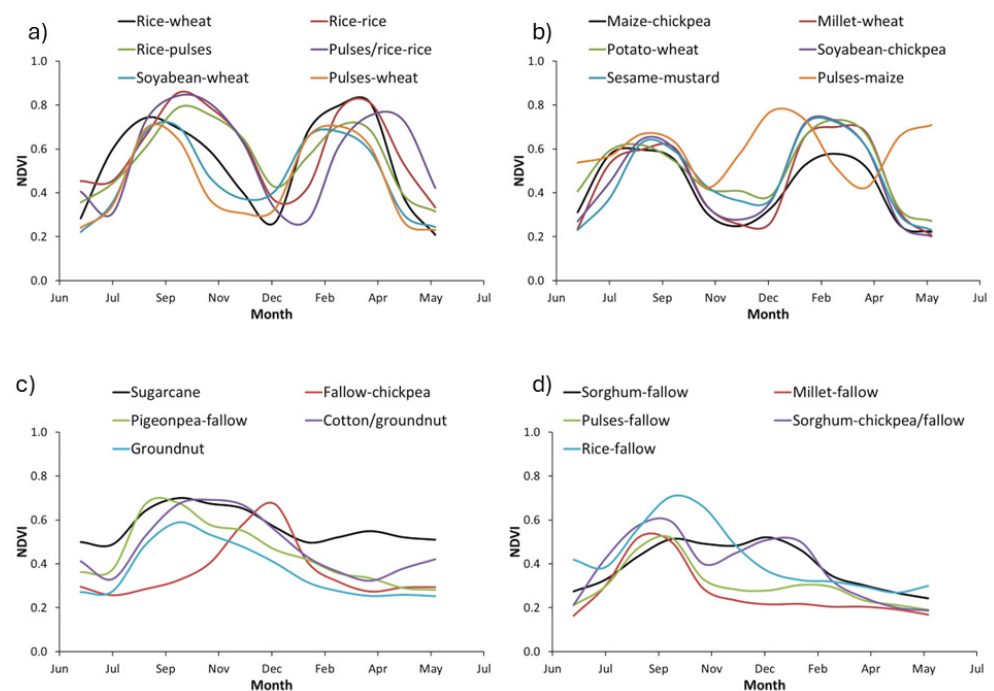


Figure 3. (a,b) Ideal Spectra Signatures of double crops (c,d) Ideal Spectra Signatures of single crop.

The spectral signature curves explain cropping systems behavior over time. Regularly, NDVI values are low during initial crop development, high through peak growth and low again at harvesting stage, due to low to high reflectance value of near infrared region band

during the crop development. In Figure 3a,b, double crop (rice-rice, rice-wheat systems, etc.) classes exhibit two peaks in a single curve, signifying that the first peak is in the start season and the second peak is in the later season. Figure 3c,d shows only a single crowning, which means that there was only a single crop (e.g., groundnut-fallow, sorghum-fallow, etc.) in a crop year. Depending on the NDVI values and ground data, we labeled classes as a combination of crop intensity and crop names.

3.2.2. Class Spectra Signatures (CSS)

Class spectra signatures (Figure 4a) were generated for the 100 classes (clusters) from unsupervised classification (K-means) of the 16-day NDVI temporal data. The signatures were generated for every individual class by taking the NDVI mean of all classified pixels of each cluster for every month.

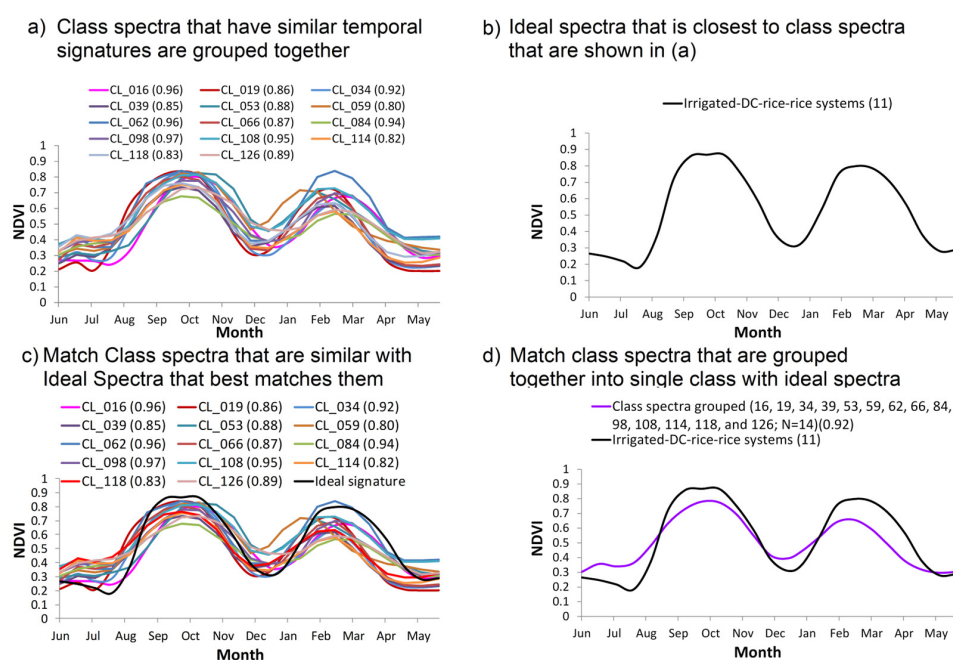


Figure 4. Matching CSS with ISS and grouping of similar classes.

3.2.3. Matching CSS with ISS to Group Classes Using SMTs

The initial 100 CSS signatures were grouped using quantitative spectral matching techniques (QSMTs), i.e., based on similar spectral signatures [53,54] (Figure 4a). The CSS (Figure 4c) signatures are then matched with the ISS (Figure 4b) and a match is determined by QSMTs with spectral correlation similarity (SCS) R-square value of 0.70 or higher are grouped and labeled as a class (Figure 4d). Classes with good visual matches both in terms of magnitude and shape of the spectral signatures are considered for class labeling.

The preliminary labeling of classes was validated, mainly by using field data, Google Earth and other secondary sources. The process was repeated to classify and label all 100 classes, leading to a finalization of classes. Wherever there was limited ground data, high-resolution data from Google Earth was used for reference. In the event of any ambiguity in the labeling of classes—e.g., some classes may not correlate with spectral signatures—such classes were reclassified using the process above [52,54].

3.3. Accuracy Assessment

Accuracy assessment was then carried out with 883 independent field points that were not used in the classification process using an error matrix. The overall classification accuracy of cropping systems and users' and producers' accuracies were calculated for each cropping system.

3.4. Sub-Pixel Areas

Highly precise area estimates from the coarse resolution imagery are only possible through sub-pixel areas (SPAs) [13,52]. This study used MOD13Q1 in which every pixel covers $250\text{ m} \times 250\text{ m}$, i.e., an area of about 6.25 ha. Full pixel areas (FPAs) are not an accurate representation of actual areas, as they may include areas falling under other LULC classes or mixed classes. On the other hand, sub-pixel areas (SPAs) involving actual area calculation, include the percentage of crop area. Therefore, areas based on SPA provide a near approximation of the cropped area.

Within the cropland class, there is a high possibility of discrepancies in the form of other LULC results. However, some classes have >50% area cropped and the proportions can vary widely. The percentage of various classes (water, cropland, etc.) is decided based on observation of ground data, photographs from ground data collection and by visualizing the field in Google Earth imagery. For example, in a rice-rice cropping system, a rice area sub pixel area (SPA), i.e., actual area is calculated based on the crop land area fraction (CAF), i.e., percent of the rice area in $250\text{ m} \times 250\text{ m}$ area of random rice field observation samples in that class. This process was carried out for each cropping system obtained. To get the actual areas, the FPA was multiplied by the CAF [55]. Since major cropping systems were mapped, the areas obtained are nearly equivalent to SPAs, with a few exceptions. Each class is evaluated for its actual area as follows:

$$\text{SPAs} = \text{FPAs} \times \text{CAFs} \quad (2)$$

4. Results

4.1. Cropping Systems

We find there are 27 major cropping systems in South Asia (Figure 5 and Table 3). Non-croplands are found in the extreme northern and western parts of South Asia and the Himalayas in the north, and are ~55% of the land cover of South Asia. The non-croplands consist mainly of deserts, mountains, glaciers and hills. The croplands are in the river valleys and vegetated plains. Around 45 percent of South Asia comprises croplands.

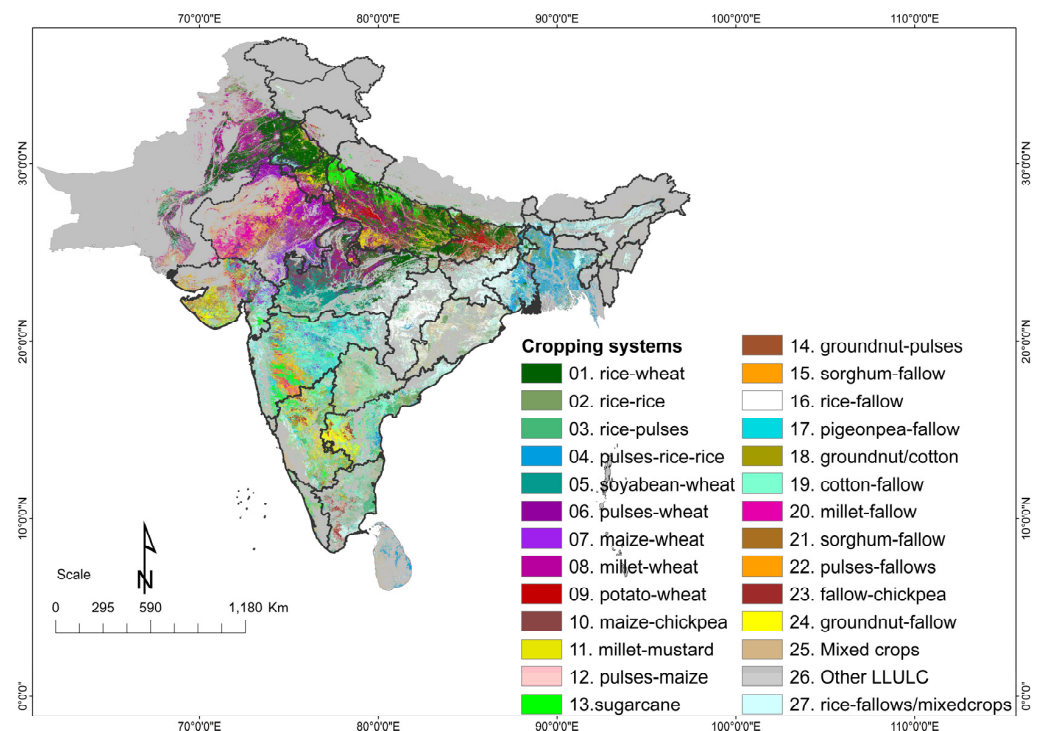


Figure 5. The distribution of 27 major cropping systems across South Asia.

Table 3. The area covered under major cropping systems of South Asia.

Cropping Systems	Sub-Pixel Area (SPA) Fractions						Full Pixel Area FPA ('000 ha)	
	Trees	Shrubs	Water	Grasses	Orchards	Other LULC		Crop Area
01. Rice-wheat	1.9	6.2	3.9	0.3	0.5	3.9	83.4	23,884
02. Rice-rice	1.7	2.5	1.5	0.4	0.0	2.9	91.1	5608
03. Rice-pulses	2.1	2.2	1.7	0.1	0.0	5.6	88.4	5967
04. Pulses/rice-rice	0.7	2.1	2.4	0.0	0.7	4.0	90.0	8537
05. Soybean-wheat	2.0	3.1	0.2	0.0	0.0	3.1	91.7	7378
06. Pulses-wheat	1.6	2.3	0.0	0.0	0.3	4.7	91.2	5007
07. Maize-wheat	1.6	2.8	0.6	0.0	1.1	4.4	89.4	6877
08. Millet-wheat	1.4	0.8	0.3	0.0	0.5	3.9	93.3	13,469
09. Maize-wheat	1.6	0.8	0.9	0.0	1.9	3.9	91.0	3193
10. Maize-chickpea	1.1	8.3	0.8	0.0	0.6	3.0	86.2	6342
11. Millet-mustard	1.7	0.6	0.0	0.0	0.4	3.8	93.4	4259
12. Pulses-maize	3.0	9.3	1.7	0.0	5.0	2.3	78.7	2740
13. Sugarcane	1.6	0.0	0.1	0.0	0.3	2.4	95.6	5509
14. Groundnut-pulses	2.1	2.7	0.9	0.0	0.0	4.4	89.9	4699
15. Sorghum-fallow	3.0	5.8	0.7	0.0	0.8	4.7	85.0	1667
16. Rice-fallow	4.8	1.6	0.4	0.0	0.0	1.8	91.4	13,414
17. Pigeon pea-fallow	3.9	10.2	0.4	0.2	4.5	11.7	69.2	10,035
18. Groundnut/cotton	1.4	1.0	0.4	0.2	0.6	2.4	94.0	4241
19. Cotton-fallow	1.9	3.9	1.3	0.5	0.0	5.0	87.3	19,045
20. Millet-fallow	2.9	2.4	0.1	0.0	0.0	2.9	91.7	4284
21. Sorghum-fallow	2.6	5.7	1.3	0.4	0.0	7.1	82.9	4991
22. Pulses-fallows	1.8	13.4	1.1	0.1	2.0	7.2	74.5	2538
23. Fallow-chickpea	0.7	22.3	0.1	0.0	4.0	1.7	71.3	1999
24. Groundnut-fallow	1.2	1.9	1.0	0.0	4.0	2.3	89.6	6251
25. Mixed crops	4.0	10.8	3.4	0.5	0.0	1.3	80.0	31,596
26. Other LULC	0.5	52.4	0.5	0.0	0.0	31.0	15.6	214,625
27. Rice-fallows/mixed crops	0.9	22.9	2.7	0.1	3.8	9.4	60.2	24,360

There are 14 double cropped cropping systems and 11 single crops cropping systems, 1 mixed crop cropping system, and 1 other land use class, i.e., non-croplands in South Asia. Each cropping system has unique crop or crop-combinations. For example, there are several cropping systems with rice as one of the crops such as rice-rice double crop (i.e., kharif season rice followed by rabi season rice), or rice-fallow system in which there is only a single rice crop (i.e., kharif season rice followed by fallow winter season rice). Some other major classes were rice-wheat, rice-pulses, sorghum-fallow, millet-fallow and mixed crops.

4.2. Spatial Distribution of Each Cropping System

There is, in general, a dominating major crop of the rainy (kharif) season such as rice together with a secondary crop in the rabi and/or zaid summer season (not common). Below, we describe our findings of fifteen major cropping systems of South Asia in greater details (Figure 6):

Rice-wheat: This is the dominant cropping system in the South Asia covering nearly 19.9 Mha stretching from Pakistan (along the Indus River basin) across into northern India (Indo-Gangetic plains) covering the states of Punjab in the west to Bihar in the east. In this system, rice crop is planted at the start of the rainy season (kharif) in June (analysis of spectral signature—Figure 3) and harvested at the end of summer monsoon season starting in August and lasting through September. As harvest progresses, NDVI reduces more gradually till it reaches a minimum and then around November wheat crop starts to emerge starting first with Bihar and ending last with those in Pakistan. Finally, wheat harvests start in March–April and they proceed much faster than rice harvests.

Rice-rice: Rice followed by a second rice crop can be observed in eastern India down to the south of India, Pakistan and in entire Bangladesh covering nearly 5.1 Mha of area. This cropping system is prevalent in irrigated lands and coastal areas. Unfortunately, the practice of mono-cropping in these regions has led to soil degradation and a deficiency in essential micronutrients. The first rice crop is in the kharif season, and sown during the

monsoon months, typically between June and July, and is ready for harvest from September to October. After harvesting the first rice crop, the same fields are used for the second rice crop, which is planted during the dry winter months of the rabi season, usually between November and December. The second rice crop harvest starts from February to March as seen in their spectral signature.

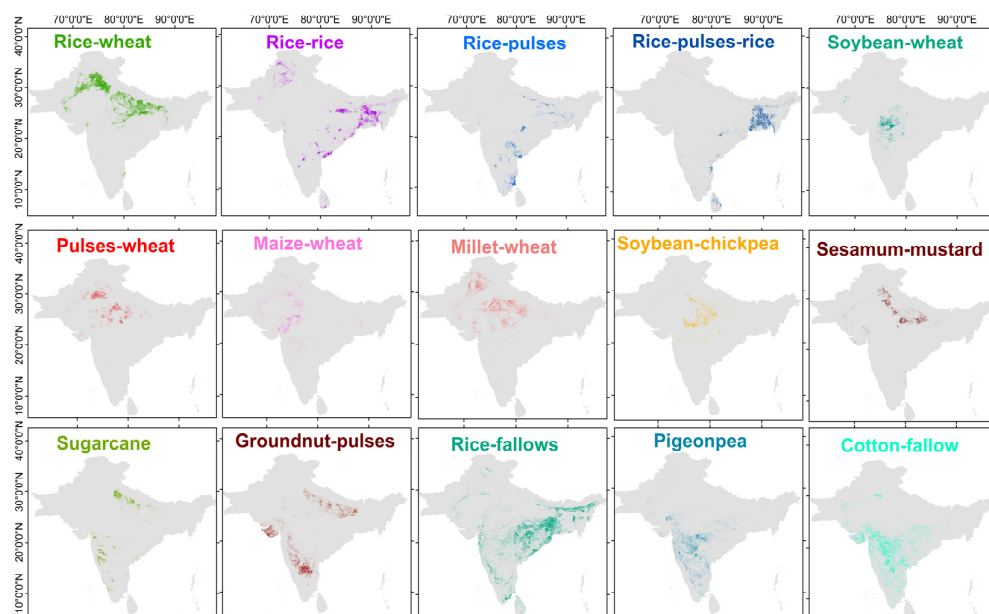


Figure 6. Maps of spatial distribution of individual major cropping systems.

Rice-pulses: Rice cultivation in rainy season and followed by pulses cultivation is observed in east to south India covering about 5.2 Mha of area. This cropping system is practiced in parts of Chhattisgarh, Odisha, Tamil Nadu and Bihar states in India. It has led to high yields of both rice and pulses. However, the challenge lies in the irregular availability of irrigation in these regions. Rice cultivation takes place during the kharif season, where the sowing of rice seeds begins from June to July and harvesting between the months of September and October. Our spectral signature shows that subsequently, pulses are sown between November and December in this cropping system regions with the matured pulses harvested between February and March. Nearly 0.3 Mha is observed in Nepal and Bangladesh and no significant area of this cropping system is present in Pakistan, Bhutan and Sri Lanka.

Rice-pulses-rice: This is the cropping system of three crops in a single crop year in which rice is followed by pulses and then by another rice crop. This cropping system is observed mostly in Bangladesh, but also in a few parts of Sri Lanka and India where irrigation coverage is excellent. The first rice crop is sown between June and July and is typically harvested from September to October. Subsequently, pulses are sown between November and December and then harvested from February to March. After the pulse harvest, preparations are made for the second rice crop to be sown in April to May, followed by the harvesting of the second rice crop from June to July. It is this latter zaid season crop that is irrigated.

Soybean-wheat: The cultivation of soybean followed by wheat is seen majorly in Madhya Pradesh state of India covering nearly 6.6 Mha of area. This system is also found in Rajasthan, and certain regions of southern Maharashtra. Soybean cultivation in India primarily occurs during the kharif season, with our spectral signature showing the sowing of soybean seeds between June and July and harvest taking place from September to October. In the subsequent rabi season, after the soybean harvest, typically occurring in October to November, fields are prepared for wheat cultivation. Wheat is sown from November to December, and the mature wheat crop is harvested between March and April. Approximately 0.1 Mha of this cropping system is observed in Pakistan, whereas there is no significant area in other countries.

Pulses–wheat: Unlike the rice-pulse-rice system, this system is concentrated in northern India and into neighboring Pakistan, spanning an area of approximately 4.5 million hectares (Table 1). It is prevalent in several states, especially northern Indian regions, including Uttar Pradesh, Madhya Pradesh, Rajasthan, Haryana and Punjab states. The usual pattern involves planting kharif pulses like chickpeas, pigeon peas and lentils during the monsoon season, followed by the rabi wheat crop. Pulses cultivation follows a specific timeline, with pulses being sown from June to August and harvested between October and November. Wheat is sown from November to December, and the mature wheat crop is ready for harvesting between March and April.

Maize-wheat: Maize followed by wheat cultivation is observed in western parts of India and Pakistan, covering nearly 6.1 Mha of area. In this cropping system, maize is the primary crop during the kharif season, while wheat takes center stage in the rabi season. This system is widely practiced in states like Uttar Pradesh, Rajasthan, Madhya Pradesh, Bihar and Punjab. A significant portion of the maize-wheat system is rainfed, which means it heavily relies on rainfall, posing a major challenge due to its unpredictability. In the kharif season of India, maize sowing is carried out between June and July, and the maize harvest occurs during September to October. Subsequently, in the rabi season that follows, wheat is sown between November and December, and the mature wheat crop is usually ready for harvesting between March and April. Approximately 0.1 Mha of this cropping system is observed in Pakistan, whereas there is no significant area in other countries.

Millet-wheat: The cultivation of millet followed by wheat is observed in northern parts of India and also in Pakistan, covering 12.5 Mha of area. These are significant cropping systems in the western part of India, particularly in the semi-arid regions of Gujarat, Rajasthan and Haryana. Wheat is cultivated as a rabi crop, while Millet is grown during the kharif season. Millet cultivation is carried out between June and July, with millet ready for harvesting in September to October. Subsequently, in the following rabi season, wheat is sown from November to December, and the mature wheat crop is typically harvested between March and April.

Soybean-chickpea: This type of cropping system is observed in the central parts of India covering nearly 5.4 Mha of area, especially in the areas of Madhya Pradesh and some areas of Uttar Pradesh states. During the kharif season in India, soybean sowing starts between June and July, with the soybean harvest typically taking place from September to October. In the subsequent rabi season, chickpeas are sown from November to December and are ready for harvesting between February and March.

Sesame-mustard: The cultivation of sesame followed by mustard is observed in Uttar Pradesh state of India covering nearly 3.9 Mha of area. The sesame-mustard cropping system is adopted in various states across India, including Rajasthan, Gujarat, Madhya Pradesh, Uttar Pradesh, Bihar and portions of Haryana and Punjab. In the kharif season, sesame cultivation starts with sowing between June and July, and the sesame crop is typically harvested from September to October. In the subsequent rabi season, Mustard is sown from November to December and is usually ready for harvesting between February and March.

Sugarcane: Sugarcane is a whole-year crop, i.e., cultivated throughout the crop year mostly in Uttar Pradesh and Maharashtra states. Sugarcane is grown in several states across India, with Uttar Pradesh, Maharashtra, Karnataka, Tamil Nadu, Andhra Pradesh and Bihar being the major sugarcane-producing states. Sugarcane is usually planted in the pre-monsoon or early monsoon season. In northern India, it is planted from March to June, while in southern India, planting can even extend into July.

Rice-fallows: Rice fallows are predominantly found in both rainfed and irrigated areas of the south Asia. The significant rainfed rice-fallows area found in India of about 11.4 Mha and mixed irrigated rice-fallows of nearly 13.3 Mha, whereas Bangladesh and Pakistan have nearly 0.5 Mha.

Pigeon pea-fallows: The pigeon pea-fallow cropping system is mainly practiced in the semi-arid and arid regions of India, including areas in Rajasthan, Gujarat, Maharashtra, Karnataka and Madhya Pradesh, covering about 6.7 Mha. Generally, depending upon the

rainfall, the sowing of pigeon pea will be done and cultivation period ranges from 6 months to more than one year in some areas.

Cotton-fallow: Cotton-fallow areas are also significantly found in India, which is about 16.2 Mha of area. This cropping systems is predominantly in states of Karnataka, Maharashtra and some parts of Gujarat. Cotton sowing happens in June-July, and harvesting takes place from October to January.

The remote sensing-based data on full-pixel crop areas of major cropping systems (Table 3) was further refined as the actual area statistics which were calculated using SPA by taking random samples of each class and identified the percentage of crop found in respective class pixels. The SPA was calculated given the possibility of non-crop pixels in crop pixels due to coarser resolution.

Sub-pixel areas in each cropping system were calculated. It was observed that on an average, 10 to 20 percent of each class contains other LULC. We calculated the sub-pixel areas for each class to get the actual area by eliminating 10–20 percent accordingly.

4.3. Country-Wise Cropping Systems

Country-wise cropping systems and their respective sub-pixel areas shows the dominant cropping sequence followed in each country (Table 4). In Pakistan, the dominant cropping systems are rice-wheat (4.3 M ha) followed by millet-wheat (3.4 M ha) and rice-rice (1.4 M ha). In Nepal, the major cropping systems are rice-wheat (0.4 M ha) and rice-pulses (0.36 M ha). In Bhutan, the cropping systems are rice-fallow (0.012 M ha) and pulses-rice-rice (0.007 M ha). In Bangladesh, the dominant cropping systems are pulses-rice-rice (3.8 M ha) followed by rice-rice (1.1 M ha), whereas in Sri Lanka, the dominant cropping system is pulses-rice-rice (0.49 M ha). In India, there are highly diversified cropping systems such as rice-wheat (15.1 M ha), rice-fallow (11.4 M ha), cotton-fallow (16.2 M ha) and rice-fallow/mixed crops (13.3 M ha), followed by a significant shared area with different cropping systems. The dominance of rice-fallow cropping systems provides opportunities for intensification with short-duration pulse crops.

Table 4. Country-wise net crop area under different cropping systems.

Cropping Systems	Net Area ('000 ha)					
	Pakistan	Nepal	Bhutan	Bangladesh	Sri Lanka	India
01. Rice-wheat	4328	420	0	2	0	15,170
02. Rice-rice	1412	4	0	1126	3	2564
03. Rice-pulses	50	365	1	399	4	4456
04. Pulses-rice-rice	30	39	7	3816	497	3293
05. Soybean-wheat	145	0	0	0	0	6620
06. Pulses-wheat	610	1	0	0	0	3955
07. Maize-wheat	826	0	0	0	0	5324
08. Millet-wheat	3406	7	0	0	53	9094
09. Potato-wheat	0	100	0	0	0	2806
10. Soybean-chickpea	123	1	0	0	0	5341
11. Sesamum-mustard	112	10	0	0	2	3854
12. Pulses-maize	0	0	0	0	0	2156
13. Sugarcane	0	76	0	0	0	5189
14. Groundnut-pulses	0	19	0	0	0	4204
15. Sorghum-fallow	0	0	0	0	0	1417
16. Rice-fallow	95	125	2	633	1	11,403
17. Pigeonpea-fallow	181	0	0	0	4	6758
18. Groundnut/cotton	13	0	0	1	1	3971
19. Cotton-fallow	393	5	1	1	2	16,231
20. Millet-fallow	740	6	1	2	6	3175
21. Sorghum-fallow	472	2	1	0	0	3661
22. Pulses-fallows	264	0	0	0	1	1625
23. Fallow-chickpea	39	0	0	0	7	1379
24. Groundnut-fallow	0	0	0	0	0	5601
25. Mixed crops	1619	403	28	864	739	21,623
26. Other LULC	9605	1940	611	843	681	19,800
27. Rice-fallows/mixed crops	406	258	12	407	239	13,349
Net cropped area	24,871	3781	664	8096	2240	184,020

4.4. Comparison of Remote Sensing-Derived Crop Area Statistics to Survey Based National Statistics

Data on area by cropping system was extracted from a remote sensing-derived cropping systems map and compared with National Agriculture Statistics (NAS) for the year 2014–15 obtained from the Department of Agriculture. The analysis reveals significant discrepancies between the reported areas in NAS and those derived from the remote sensing map for various crop combinations. Crop combinations like pigeon pea-fallow (77.56%), maize-chickpea (54.95%) and pulses-fallow (67.82%) show substantial positive differences. Conversely, soybean-wheat (−13.02%), millets-fallow (−8.91%) and millets-wheat (−3.44%) exhibit negative differences. Some combinations, such as rice-fallow (−0.99%) and sugarcane (6.46%), show minimal differences, indicating a varying level of alignment between reporting and mapping methods (Figure 7).

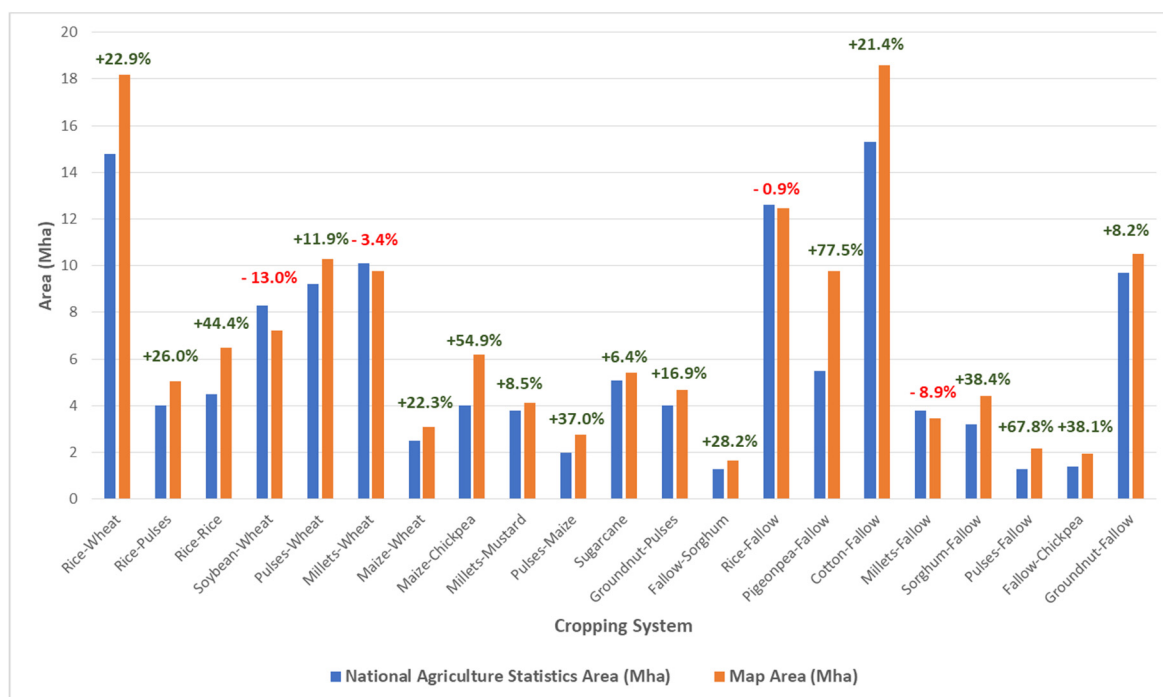


Figure 7. Comparison of remote sensing-derived crop areas with that from national statistics.

The accuracy assessment was calculated for identified cropping systems with 883 independent ground points. Overall classification accuracy was observed to be 76.59 percent, with kappa coefficient of 0.75. User and producer accuracies of major cropping systems ranged from 70 per cent to 90 percent, whereas mixed cropping system showed less accuracy ranging from 50 percent to 70 percent.

The major rice-wheat cropping system showed a user accuracy of 89 percent and producer accuracy of 72 percent, and pulses-wheat systems revealed a user accuracy of 92 percent and producer accuracy of 100 percent. Likewise, each cropping system was validated using validation points, their individual class accuracies and kappa coefficient determined (Table 5). Due to domination of small-holding farms and mixed crops in major areas of south Asia, the accuracy of some of the minor cropping systems was lower. The mapping accuracy of such cropping systems can be increased by utilizing high resolution satellite data along with more extensive ground data collection to build better models.

Table 5. Accuracy assessment of the croplands product by error matrix method.

Classified Data	Row Total	Reference Total	Classified Total	Number Correct	Producer Accuracy (%)	User Accuracy (%)	Kappa
01. Rice-wheat	46	46	37	33	72	89	0.89
02. Rice-rice	88	88	57	50	57	88	0.86
03. Rice-pulses	51	51	52	35	69	67	0.65
04. Pulses/rice-rice	107	107	106	95	89	90	0.88
05. Soybean-wheat	33	33	35	29	88	83	0.82
06. Pulses-wheat	22	22	24	22	100	92	0.91
07. Maize-wheat	24	24	24	22	92	92	0.91
08. Millet-wheat	38	38	39	36	95	92	0.92
09. Potato-wheat	13	13	14	11	85	79	0.75
10. Maize-chickpea	14	14	15	13	93	87	0.86
11. Millet-mustard	20	20	11	11	55	100	1.00
12. Pulses-maize	10	10	12	10	100	83	0.67
13. Sugarcane	17	17	12	11	65	92	0.92
14. Groundnut-pulses	15	15	20	12	80	60	0.59
15. Sorghum-fallow	18	18	15	14	78	93	0.93
16. Rice-fallow	58	58	41	26	45	63%	0.61
17. Pigeonpea-fallow	27	27	38	22	81	58	0.57
18. Groundnut/cotton	15	15	15	8	53	53	0.53
19. Cotton-fallow	43	43	48	33	77	69	0.67
20. Millet-fallow	13	13	13	13	100	100	1.00
21. Sorghum-fallow	16	16	14	11	69	79	0.78
22. Pulses-fallows	11	11	10	10	91	100	1.00
23. Fallow-chickpea	16	16	17	16	100	94	0.94
24. Groundnut-fallow	14	14	18	12	86	67	0.66
25. Mixed crops	55	55	50	41	75	82	0.81
26. Other LULC	61	61	91	52	85	57	0.54
27. Rice-fallow/mixed crops	38	38	55	38	100	69	0.68
Total	883	883	883	686	Overall accuracy = 76.59%;	Kappa = 0.7545	

5. Discussion

While the classification of irrigated, homogenous crops such as rice and wheat were relatively easy throughout South Asia, identification of rainfed crops like groundnut and pulses was difficult. Further, cropping patterns in most regions of south Asia vary widely, with a high possibility of mixed crops. In India and Bangladesh, rice is the major irrigated crop and cultivated in large homogenous extent, whereas in Pakistan, wheat is the major irrigated crop, comprising more than 25 percent of all crops. Rice and wheat cropping system areas could be identified and classified more correctly. The identification of other crops mainly depends upon extensive ground data, their ideal signatures and crop phenology. Western South Asia comprising Afghanistan and Pakistan has large tracts of uncultivated area, whereas eastern South Asia, i.e., northeastern India, contains hill areas and the north part of south Asia contains ice glaciers. Crop identification in hilly regions was affected by shadows and different cropping patterns. Nearly 26 percent of South Asian cropland consists of double crops (i.e., rainy and winter season crops). Double crops in irrigated areas were identified using spectral curves and ground data. Only 45 percent of the total area in south Asia was under cultivation, with other LULC comprising mainly deserts, glaciers and hilly areas.

Knowledge of regional cropping systems is essential to maximize land productivity and improve crop production towards the objective of sustainable agriculture. Of late, high-intensity cropping practices and overexploitation of resources have resulted in unsustainable agriculture. The 27 cropping systems identified in this study cover all major

and dominant agricultural practices in the region. These novel information products can serve as baseline data for developing sustainable agriculture solutions. When integrated with thematic layers such as weather, soil, groundwater availability and land degradation in GIS environments, they can unlock opportunities to develop action-oriented solutions to improve the performance of agriculture systems. It is also possible to produce maps with finer granularity using Sentinel data of 10 m resolution once more ground level data are collected. Sustainable agriculture and food system solutions need such innovative information products, which are potentially the low-hanging benefits from modern remote sensing technology.

Policy Implications: Cropping system maps and statistics form basic inputs for formulating sustainable agriculture plans to optimize land productivity. The major challenges of agriculture in South Asia are food security, income security and climate resilience, which can be addressed only through systematic efforts to optimize crop patterns and resource consumption in producing crops. The maps of cropping systems can now be superimposed on resources and climatology data layers to offer deeper insights to decision-makers on the efficiency of the current agricultural systems and to prioritize critical areas for immediate interventions. The design and implementation of such interventions needs a strong base of data and information on cropping systems and related analytics that our maps will now provide. These interventions will involve both management and structural measures at the grass root level, and may involve certain incentives and investments, but cannot proceed without understanding the entire cropping system of the local area. Specifically, the government of India's flagship projects on water use efficiency in agriculture, the National Food Security Mission (NFSM) and Agroforestry development mission will become more effective when cropping systems information is integrated within their design and implementation plans. The cropping system determines multiple ecosystem services, pest predation and water quality. For example, the development of agroforestry plans in a region should take into account the existing cropping system. Carbon sequestration and carbon emission potentials of croplands are directly related to the cropping systems followed in a region. Therefore, any effort towards achieving carbon neutral agroecosystems will fundamentally get guided by cropping system practices.

Policymakers across South Asia will find our cropping system maps to be quite useful, since they provide a thorough understanding of the geographical distribution of various crops within an area. These maps will help with all governmental planning of resource allocation, making investments in pest management, irrigation and crop-specific subsidies more effective. Furthermore, they are crucial in guaranteeing food security since they enable policymakers to evaluate the yield of vital food crops and create plans for agricultural output diversification. By highlighting regions with significant production potential for particular crops, cropping sequence type maps will also aid in market growth and strengthen local and regional economies. They also aid in the identification of vulnerable regions that require protection, the evaluation of the effects of farming on natural resources and the development of sustainable agricultural policy. All things considered, these maps are invaluable resources that support the development of evidence-based policies and well-informed decisions about a variety of aspects of land use and agriculture.

6. Conclusions

Knowledge of regional cropping systems is essential to maximize land productivity and improve crop production towards the objective of sustainable agriculture. Of late, high-intensity cropping practices and overexploitation of resources have resulted in unsustainable agriculture.

This study has developed a new geospatial application in the agriculture sector to address crop planning and sustainable agriculture practices.

Remote sensing imagery from MODIS 250 m was used to generate maps and statistics on different cropping systems practiced in South Asia. The 27 cropping systems identified in this study cover all major and dominant agricultural practices in the region. These novel

information products can serve as baseline data for developing sustainable agriculture solutions. When integrated with thematic layers such as weather, soil, groundwater availability and land degradation in GIS environments, they can unlock numerous opportunities to develop action-oriented solutions to improve the performance of agriculture systems. It is also possible to produce maps with finer granularity using Sentinel data of 10 m resolution. Sustainable agriculture and food system solutions need such innovative information products, which are low-hanging benefits from modern remote sensing technology.

Author Contributions: M.K.G., C.S.M. and D.K.R.: conceptualization, methodology, investigation, developing algorithms, image analysis, ground data collection, writing—reviewing and editing; P.P.: validation, writing, testing machine learning algorithms; C.S.M., Y.T. and D.M.K.: investigation, formal analysis, accuracy assessment and editing; I.M.: ground data collection; S.K.D.: agricultural statistics; Y.T.: review and editing. All authors have read and agreed to the published version of the manuscript.

Funding: This study was funded by the Japan Fund for Prosperous and Resilient Asia and the Pacific financed by the Government of Japan through the Asian Development Bank (ADB) and Mahalano-bis National Crop Forecasting Centre (MNCFC). DKR was funded with support from the Institute on the Environment and WRI Land & Carbon Lab grant number G3275. Land & Carbon Lab is convened by World Resources Institute and the Bezos Earth Fund.

Data Availability Statement: The classification of cropping systems in this study was performed on the local computer and Google Earth Engine. The code utilized is available at <https://github.com/ICRISAT-GBDS/South-Asia-Cropping-Systems.git> (accessed on 17 May 2024).

Acknowledgments: Our thanks go to Prasad S. Thenkabail, Anthony Whitbread, ML Jat and Partha Saradhi Teluguntla for their valuable comments and support.

Conflicts of Interest: The authors declare no conflicts of interest.

References

- Connor, D.J.; Loomis, R.S.; Cassman, K.G. *Crop Ecology: Productivity and Management in Agricultural Systems*; Cambridge University Press: Cambridge, UK, 2011.
- Yang, T.; Siddique, K.H.; Liu, K. Cropping systems in agriculture and their impact on soil health—A review. *Glob. Ecol. Conserv.* **2020**, *23*, e01118. [[CrossRef](#)]
- Mahlayeye, M.; Darvishzadeh, R.; Nelson, A. Cropping Patterns of Annual Crops: A Remote Sensing Review. *Remote Sens.* **2022**, *14*, 2404. [[CrossRef](#)]
- Garnett, T.; Appleby, M.; Balmford, A.; Bateman, I.; Benton, T.; Bloomer, P.; Burlingame, B.; Dawkins, M.; Dolan, L.; Fraser, D. Sustainable intensification in agriculture: Premises and policies. *Science* **2013**, *341*, 33–34. [[CrossRef](#)] [[PubMed](#)]
- Gray, J.; Friedl, M.; Frolking, S.; Ramankutty, N.; Nelson, A.; Gumma, M. Mapping Asian Cropping Intensity with MODIS. *IEEE J. Sel. Top. Appl. Earth Obs. Remote Sens.* **2014**, *7*, 3373–3379. [[CrossRef](#)]
- Boryan, C.; Yang, Z.; Mueller, R.; Craig, M. Monitoring US agriculture: The US Department of Agriculture, National Agricultural Statistics Service, Cropland Data Layer Program. *Geocarto Int.* **2011**, *26*, 341–358. [[CrossRef](#)]
- Khan, A.; Hansen, M.C.; Potapov, P.; Stehman, S.V.; Chatta, A.A. Landsat-based wheat mapping in the heterogeneous cropping system of Punjab, Pakistan. *Int. J. Remote Sens.* **2016**, *37*, 1391–1410. [[CrossRef](#)]
- Skakun, S.; Franch, B.; Vermote, E.; Roger, J.-C.; Becker-Reshef, I.; Justice, C.; Kussul, N. Early season large-area winter crop mapping using MODIS NDVI data, growing degree days information and a Gaussian mixture model. *Remote Sens. Environ.* **2017**, *195*, 244–258. [[CrossRef](#)]
- Seinn, S.; Ahmad, M.; Thapa, G.; Shrestha, R. Farmers Adaptation to Rainfall Variability and Salinity through Agronomic Practices in Lower Ayeyarwady Delta, Myanmar. *J. Earth Sci. Clim. Chang.* **2015**, *6*, 2157–7617.
- Parr, J.; Stewart, B.; Hornick, S.; Singh, R. Improving the sustainability of dryland farming systems: A global perspective. In *Advances in Soil Science*; Springer: Berlin/Heidelberg, Germany, 1990; pp. 1–8.
- Salvati, L.; Kosmas, C.; Kairis, O.; Karavitis, C.; Acikalin, S.; Belgacem, A.; Solé-Benet, A.; Chaker, M.; Fassouli, V.; Gokceoglu, C. Unveiling soil degradation and desertification risk in the Mediterranean basin: A data mining analysis of the relationships between biophysical and socioeconomic factors in agro-forest landscapes. *J. Environ. Plan. Manag.* **2015**, *58*, 1789–1803. [[CrossRef](#)]
- Feyisa, G.L.; Palao, L.K.; Nelson, A.; Gumma, M.K.; Paliwal, A.; Win, K.T.; Nge, K.H.; Johnson, D.E. Characterizing and mapping cropping patterns in a complex agro-ecosystem: An iterative participatory mapping procedure using machine learning algorithms and MODIS vegetation indices. *Comput. Electron. Agric.* **2020**, *175*, 105595. [[CrossRef](#)]

13. Gumma, M.K.; Thenkabail, P.S.; Teluguntla, P.; Rao, M.N.; Mohammed, I.A.; Whitbread, A.M. Mapping rice-fallow cropland areas for short-season grain legumes intensification in South Asia using MODIS 250 m time-series data. *Int. J. Digit. Earth* **2016**, *9*, 981–1003. [[CrossRef](#)]
14. Thenkabail, P.S.; Hanjra, M.A.; Dheeravath, V.; Gumma, M. A holistic view of global croplands and their water use for ensuring global food security in the 21st century through advanced remote sensing and non-remote sensing approaches. *Remote Sens.* **2010**, *2*, 211–261. [[CrossRef](#)]
15. Mao, Z.-H.; Deng, L.; Duan, F.-Z.; Li, X.-J.; Qiao, D.-Y. Angle effects of vegetation indices and the influence on prediction of SPAD values in soybean and maize. *Int. J. Appl. Earth Obs. Geoinf.* **2020**, *93*, 102198. [[CrossRef](#)]
16. Xu, J.; Zhu, Y.; Zhong, R.; Lin, Z.; Xu, J.; Jiang, H.; Huang, J.; Li, H.; Lin, T. DeepCropMapping: A multi-temporal deep learning approach with improved spatial generalizability for dynamic corn and soybean mapping. *Remote Sens. Environ.* **2020**, *247*, 111946. [[CrossRef](#)]
17. Wang, M.; Liu, Z.; Ali Baig, M.H.; Wang, Y.; Li, Y.; Chen, Y. Mapping sugarcane in complex landscapes by integrating multi-temporal Sentinel-2 images and machine learning algorithms. *Land Use Policy* **2019**, *88*, 104190. [[CrossRef](#)]
18. Dong, J.; Xiao, X. Evolution of regional to global paddy rice mapping methods: A review. *ISPRS J. Photogramm. Remote Sens.* **2016**, *119*, 214–227. [[CrossRef](#)]
19. Xiao, X.; Boles, S.; Liu, J.; Zhuang, D.; Froelking, S.; Li, C.; Salas, W.; Moore III, B. Mapping paddy rice agriculture in southern China using multi-temporal MODIS images. *Remote Sens. Environ.* **2005**, *95*, 480–492. [[CrossRef](#)]
20. Zhang, G.; Xiao, X.; Biradar, C.M.; Dong, J.; Qin, Y.; Menarguez, M.A.; Zhou, Y.; Zhang, Y.; Jin, C.; Wang, J. Spatiotemporal patterns of paddy rice croplands in China and India from 2000 to 2015. *Sci. Total Environ.* **2017**, *579*, 82–92. [[CrossRef](#)]
21. Gumma, M.K.; Nelson, A.; Thenkabail, P.S.; Singh, A.N. Mapping rice areas of South Asia using MODIS multitemporal data. *J. Appl. Remote Sens.* **2011**, *5*, 053547. [[CrossRef](#)]
22. Sun, H.; Xu, A.; Lin, H.; Zhang, L.; Mei, Y. Winter wheat mapping using temporal signatures of MODIS vegetation index data. *Int. J. Remote Sens.* **2012**, *33*, 5026–5042. [[CrossRef](#)]
23. Huke, R.E. *Rice Area by Type of Culture: South, Southeast, and East Asia*; International Rice Research Institute: Los Banos, CA, USA; Laguna, Philippines, 1982.
24. Huke, R.E.; Huke, E.H. *Rice Area by Type of Culture: South, Southeast, and East Asia, A Revised and Updated Data Base*; International Rice Research Institute: Los Banos, CA, USA; Laguna, Philippines, 1997.
25. Aselman, I.; Crutzen, P.J. Global distribution of natural freshwater wetlands and rice paddies, their net primary productivity, seasonality and possible methane emissions. *J. Atmos. Chem.* **1989**, *8*, 307–358. [[CrossRef](#)]
26. Xiao, X.; Boles, S.; Froelking, S.; Li, C.; Babu, J.Y.; Salas, W.; Moore Iii, B. Mapping paddy rice agriculture in South and Southeast Asia using multi-temporal MODIS images. *Remote Sens. Environ.* **2006**, *100*, 95–113. [[CrossRef](#)]
27. Takeuchi, W.; Yasuoka, Y. Sub-pixel mapping of rice paddy fields over Asia using MODIS time series. In *Remote Sensing of Global Croplands for Food Security (Remote Sensing Applications Series)*; Thenkabail, P., Lyon, J.G., Turrall, H., Biradar, C., Thenkabail, P., Eds.; CRC Press: Boca Raton, FL, USA, 2009.
28. Sun, H.; Huang, J.; Huete, A.R.; Peng, D.; Zhang, F. Mapping paddy rice with multi-date moderate-resolution imaging spectroradiometer (MODIS) data in China. *J. Zhejiang Univ. Sci. A* **2009**, *10*, 1509–1522. [[CrossRef](#)]
29. Froelking, S.; Yeluripati, J.B.; Douglas, E. New district-level maps of rice cropping in India: A foundation for scientific input into policy assessment. *Field Crops Res.* **2006**, *98*, 164–177. [[CrossRef](#)]
30. Froelking, S.; Qiu, J.; Boles, S.; Xiao, X.; Liu, J.; Zhuang, Y.; Li, C.; Qin, X. Combining remote sensing and ground census data to develop new maps of the distribution of rice agriculture in China. *Glob. Biogeochem. Cycles* **2002**, *16*, 3801–3810. [[CrossRef](#)]
31. Thenkabail, P.S.; Biradar, C.M.; Noojipady, P.; Dheeravath, V.; Li, Y.; Velpuri, M.; Gumma, M.; Gangalakunta, O.R.P.; Turrall, H.; Cai, X.; et al. Global irrigated area map (GIAM), derived from remote sensing, for the end of the last millennium. *Int. J. Remote Sens.* **2009**, *30*, 3679–3733. [[CrossRef](#)]
32. Badhwar, G.D. Automatic corn-soybean classification using landsat MSS data. I. Near-harvest crop proportion estimation. *Remote Sens. Environ.* **1984**, *14*, 15–29. [[CrossRef](#)]
33. Lobell, D.B.; Asner, G.P.; Ortiz-Monasterio, J.I.; Benning, T.L. Remote sensing of regional crop production in the Yaqui Valley, Mexico: Estimates and uncertainties. *Agric. Ecosyst. Environ.* **2003**, *94*, 205–220. [[CrossRef](#)]
34. Thiruvengadachari, S.; Sakthivadivel, R. *Satellite Remote Sensing for Assessment of Irrigation System Performance: A Case Study in India*; Research Report 9; International Irrigation Management Institute: Colombo, Sri Lanka, 1997.
35. Thenkabail, P.S. Global Croplands and their Importance for Water and Food Security in the Twenty-first Century: Towards an Ever Green Revolution that Combines a Second Green Revolution with a Blue Revolution. *Remote Sens.* **2010**, *2*, 2305–2312. [[CrossRef](#)]
36. Dheeravath, V.; Thenkabail, P.S.; Chandrakantha, G.; Noojipady, P.; Reddy, G.P.O.; Biradar, C.M.; Gumma, M.K.; Velpuri, M. Irrigated areas of India derived using MODIS 500 m time series for the years 2001–2003. *ISPRS J. Photogramm. Remote Sens.* **2010**, *65*, 42–59. [[CrossRef](#)]
37. Goetz, S.J.; Varlyguin, D.; Smith, A.J.; Wright, R.K.; Prince, S.D.; Mazzacato, M.E.; Tringe, J.; Jantz, C.; Melchoir, B. Application of Multitemporal Landsat Data to Map and Monitor Land Cover and Land Use Change in the Chesapeake Bay Watershed. In *Analysis of Multi-Temporal Remote Sensing Images*; Smits, P., Bruzzone, L., Eds.; World Scientific Publishers: Singapore, 2024; pp. 223–232.

38. Thenkabail, P.S.; Schull, M.; Turrall, H. Ganges and Indus river basin land use/land cover (LULC) and irrigated area mapping using continuous streams of MODIS data. *Remote Sens. Environ.* **2005**, *95*, 317–341. [[CrossRef](#)]
39. Velpuri, N.M.; Thenkabail, P.S.; Gumma, M.K.; Biradar, C.B.; Noojipady, P.; Dheeravath, V.; Yuanjie, L. Influence of Resolution in Irrigated Area Mapping and Area Estimations. *Photogramm. Eng. Remote Sens.* **2009**, *75*, 1383–1395. [[CrossRef](#)]
40. Varlyguin, D.; Wright, R.; Goetz, S.J.; Prince, S.D. Advances in Land Cover Classification: A Case Study from the Mid-Atlantic Region. In Proceedings of the American Society for Photogrammetry and Remote Sensing, St. Louis, MO, USA, 23–27 April 2001; Volume 7. Available online: <https://citeseerx.ist.psu.edu/document?repid=rep1&type=pdf&doi=278fb1793b69fd19ffad89f70f846cf39dfdbf6f> (accessed on 11 February 2024).
41. Knight, J.F.; Lunetta, R.L.; Ediriwickrema, J.; Khorram, S. Regional Scale Land-Cover Characterization using MODIS-NDVI 250 m Multi-Temporal Imagery: A Phenology Based Approach. *GISci. Remote Sens.* **2006**, *43*, 1–23. [[CrossRef](#)]
42. Biggs, T.W.; Thenkabail, P.S.; Gumma, M.K.; Scott, C.A.; Parthasaradhi, G.R.; Turrall, H.N. Irrigated area mapping in heterogeneous landscapes with MODIS time series, ground truth and census data, Krishna Basin, India. *Int. J. Remote Sens.* **2006**, *27*, 4245–4266. [[CrossRef](#)]
43. Gaur, A.; Biggs, T.W.; Gumma, M.K.; Parthasaradhi, G.; Turrall, H. Water scarcity effects on equitable water distribution and land use in Major Irrigation Project—A Case study in India. *J. Irrig. Drain. Eng.* **2008**, *134*, 26–35. [[CrossRef](#)]
44. Gumma, M.K.; Thenkabail, P.S.; Muralikrishna, I.V.; Velpuri, M.N.; Gangadhararao, P.T.; Dheeravath, V.; Biradar, C.M.; Acharya Nalan, S.; Gaur, A. Changes in agricultural cropland areas between a water-surplus year and a water-deficit year impacting food security, determined using MODIS 250 m time-series data and spectral matching techniques, in the Krishna River basin (India). *Int. J. Remote Sens.* **2011**, *32*, 3495–3520. [[CrossRef](#)]
45. Sakamoto, T.; Van Nguyen, N.; Kotera, A.; Ohno, H.; Ishitsuka, N.; Yokozawa, M. Detecting temporal changes in the extent of annual flooding within the Cambodia and the Vietnamese Mekong Delta from MODIS time-series imagery. *Remote Sens. Environ.* **2007**, *109*, 295–313. [[CrossRef](#)]
46. Ratana, P.; Huete, A.R.; Yin, Y.; Jacobson, A. Interrelationship among among MODIS vegetation products across an Amazon Eco-climatic gradient. In Proceedings of the Geoscience and Remote Sensing Symposium, 2005, IGARSS'05, Proceedings. Seoul, Republic of Korea, 29 July 2005; IEEE International: Piscataway, NJ, USA, 2005; pp. 3009–3012.
47. Becerra, J.; Alvalá, R.; Berlato, M.; Molion, L.; Berri, G.; Bertossa, G.; Bertagnolli, C.; Peres, R.; Ferreira, N.; Schuch, N. Detection of Tropical Savannah (Cerrado) Physiognomies in the Legal Amazon by the Application of the Vegetation and Moisture Indices with MODIS Time Series Data. In Proceedings of the 8th International Conference on Southern Hemisphere Meteorology and Oceanography (ICSHMO), Foz de Iguaçu, Brazil, 24–28 April 2006; pp. 861–868.
48. Chandrasekar, K.; Sesha Sai, M.V.R.; Roy, P.S.; Dwevedi, R.S. Land Surface Water Index (LSWI) response to rainfall and NDVI using the MODIS Vegetation Index product. *Int. J. Remote Sens.* **2010**, *31*, 3987–4005. [[CrossRef](#)]
49. Choice, H. Agroecological Zones. 2009. Available online: <http://harvestchoice.org/production/biophysical/agroecology> (accessed on 1 May 2010).
50. WorldBank. Rural Population (% of Total Population)—South Asia. 2021. Available online: <https://data.worldbank.org/indicator/SP.RUR.TOTL.ZS?locations=8S> (accessed on 25 March 2023).
51. Thenkabail, P.S.; Biradar, C.M.; Noojipady, P.; Dheeravath, V.; Li, Y.J.; Velpuri, M.; Reddy, G.; Cai, X.; Gumma, M.; Turrall, H. *A Global Irrigated Area Map (GIAM) Using Remote Sensing at the End of the Last Millennium*; International Water Management Institute: Colombo, Sri Lanka, 2008.
52. Gumma, M.K.; Thenkabail, P.S.; Maunahan, A.; Islam, S.; Nelson, A. Mapping seasonal rice cropland extent and area in the high cropping intensity environment of Bangladesh using MODIS 500m data for the year 2010. *ISPRS J. Photogramm. Remote Sens.* **2014**, *91*, 98–113. [[CrossRef](#)]
53. Homayouni, S.; Roux, M. Material Mapping from Hyperspectral Images using Spectral Matching in Urban Area. In Proceedings of the IEEE Workshop in Honour of Prof. Landgrebe, Washington, DC, USA, 6 October 2003.
54. Thenkabail, P.; Gangadhararao, P.; Biggs, T.; Gumma, M.; Turrall, H. Spectral matching techniques to determine historical land-use/land-cover (LULC) and irrigated areas using time-series 0.1-degree AVHRR Pathfinder datasets. *Photogramm. Eng. Remote Sens.* **2007**, *73*, 1029–1040.
55. Thenkabail, P.S.; Biradar, C.M.; Noojipady, P.; Cai, X.; Dheeravath, V.; Li, Y.; Velpuri, M.; Gumma, M.; Pandey, S. Sub-pixel area calculation methods for estimating irrigated areas. *Sensors* **2007**, *7*, 2519–2538. [[CrossRef](#)]

Disclaimer/Publisher’s Note: The statements, opinions and data contained in all publications are solely those of the individual author(s) and contributor(s) and not of MDPI and/or the editor(s). MDPI and/or the editor(s) disclaim responsibility for any injury to people or property resulting from any ideas, methods, instructions or products referred to in the content.